Chemical Concepts

International Journal of Chemical Concepts
ISSN:2395-4256 **www.chemconsai.com**
Vol.03, No.01, pp 180-188, 2017

Photocatalytic degradation of methylene blue dye using ZnO thin films

S.Shankar, M.Saroja, M.Venkatachalam, G.Parthasarathy

Thin film centre, Department of Electronics, Erode Arts and Science College, Erode, Tamil Nadu, India.

Abstract : Zinc oxide thin films were deposited on glass substrates using sol gel spin coating method. Zinc acetate dihydrate was used as a starting material. Isoproponol and monoethanolamine were used as the solvent and stabilizer respectively. The prepared solution was dropped on the cleaned glass substrates and the substrates were rotated at 2000 rpm for 20s and the ZnO thin films were prepared by repeated coating. The prepared thin films were annealed at 250,350 and 450^{o}C. The annealed films were characterized by x-ray diffraction (XRD), scanning electron microscopy (SEM), ultraviolet – visible spectrophotometer (UV-Vis), photoluminescence spectroscopy (PL). Photocatalytic activities of ZnO thin films annealed at 450^{o}C have been examined towards the photo degradation of methylene blue by varying degradation time and area of catalysist. A maximum efficiency of 90.4% is reported using low watt (8W) UV source.
Keywords : ZnO thin films, spin coating method, photocatalytic activity.

Introduction

The removal of organic pollutants in waste water using semiconductor photocatalysts has attracted a lot of attention as an important issue on environmental protection[1,2,3,4,5]. Wide and direct band gap semiconductors are of great interest in photo catalysis with Zinc oxide (ZnO) representing a perspective field. ZnO a wide and direct band gap (3.37 eV) semiconductor with a large exciton binding energy (60 meV)[6] has already been widely used in piezoelectric transducers, gas sensors, optical waveguides, transparent conductive films, varistors, solar cell windows, bulk acoustic wave devices and photo catalytic activities[7,8,9,10,11,12]. Many attempts have been made to study and compare the photo catalytic activity of different semiconductors and found ZnO to be one of the most effective catalysts. Nanostructure ZnO has attracted more interests because of its considerable photocatalytic efficiency and good stability[13].Several works report the synthesis and high photocatalytic efficiency of ZnO nanoparticles, powders and colloids[14,15,16]. But for the water treatment applications, ZnO thin films are preferred to avoid the separation of the catalyst after the degradation process. ZnO films have been prepared by various methods of film depositions, which include r.f sputtering[17], pulsed laser deposition[18], laser molecular beam epitaxy[19], electron beam evaporation[20], spray pyrolysis[21], sol-gel process [22-29] etc. The sol gel process has distinct advantages over the other techniques due to excellent compositional control, homogeneity on the molecular level due to the mixing of liquid precursors, and lower crystallization temperature [30].

In the present work, ZnO thin films were prepared on glass substrate by the sol gel spin coating method using homogeneous and stable zinc acetate dihydrate, isoproponal and monoethanolamine. The structural and optical properties of the samples were studied. The prepared ZnO thin films were used as effective semiconductor catalysts for photo degradation of methylene blue dye in aqueous solution. The degradation efficiencies of ZnO films are reported.

Experimental methods

Zinc acetate dihydrate ($Zn(CH_3COO)_2 .2H_2O$), monoethanolamine(MEA,$H_2N(CH_2CH_2OH)$), isopropanol ($(CH_3)_2CHOH$, Merck) were used as starting material, stabilizer and solvent to prepare the coating solution. All the chemicals used in the experiment were of analytical grade and were used without further purification. The molar ratio of MEA to zinc acetate dihydrate was maintained at 1.0 and the concentration of zinc acetate dihydrate was 0.5 mol/l. Zinc acetate dihydrate was first dissolved in isopropanol, then MEA was added drop by drop in the solution. The resultant solution was stirred at 50^0C for 2h to yield a clear and homogeneous solution. Finally the solution was aged at room temperature for 24h.

The prepared solution was dropped on the cleaned glass substrates and the substrates were rotated at 2000 rpm for 20s (Apex Instruments Co SCU -2008C) and the ZnO thin films were prepared by repeated coating. After each coating films were heated at 200°C for 10 min to evaporate the solvent and the organic residuals (named as pre-heat treatment). After the pre-heat treatment, the ZnO thin films were allowed to cool to room temperature to avoid crakes. The spin-coating and pre-heating process were repeated for ten times. For crystallization, the ZnO thin films were annealed in a furnace in air atmosphere at 250,350 and 450°C for 60 minutes and allowed to cool to room temperature gradually. The annealing is to convert the organic coating containing Zn^{2+} into its respective oxide.

Methyelene blue ($C_{16}H_{18}N_3SCI$), a widely used dye, was employed as a representative dye pollutant to evaluate the photocatalytic activity of ZnO thin films. The samples were suspended in 20ml methyelene blue solution and were irradiated with 8W UV lamp placed at a distance of 4.0 cm. The photocatalytic activity was studied by varying the irradiation time and the area of catalyst.

Results and Discussion

Structural studies

The crystalline structure of samples annealed at different temperatures was analyzed by XRD. Figure 1 shows the XRD diffraction pattern of ZnO thin films annealed at different temperatures of 250, 350 and 450°C. The very strong (100),(002) and (101) peaks corresponding to the 2θ values of 31.80°, 34.442° and 36.278o and the very weak (102), (110), (103), and (112) peaks corresponding to the 2θ values of 47.62°,56.7°,62.94°, and 68.0° are in good agreement with the standard JCPDS card (36-1451) for hexagonal wurtzite ZnO. The relative intensity of the peaks tends to increase with an increase in the annealing temperature. The increase in peak intensities indicates an improvement in the crystallinity of the films. Sharp peaks with maximum intensity were observed for films annealed at 450°C. As seen from the XRD pattern (002) peak intensity was weaker than that of the (100) and (101) peaks because annealing at 450°C results in increasing in number of oxygen defects.

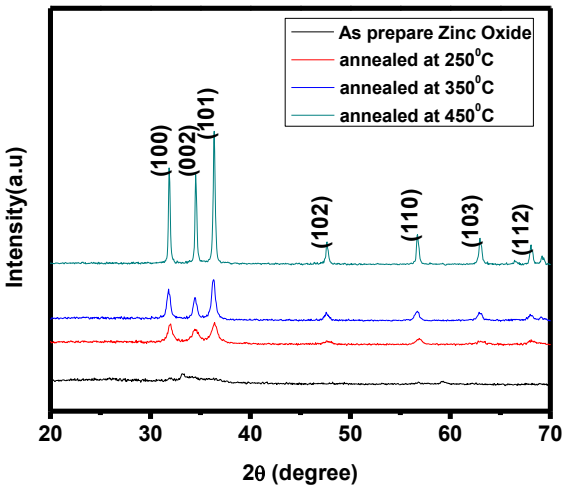

Figure 1. X-ray diffraction patterns of ZnO thin films annealed at different temperatures.

The grain size of the ZnO thin films has been estimated from FWHM of (002) diffraction peak using the Scherrer formula[31]

$d = k\lambda / \beta\cos\theta$

where λ is the X-ray wavelength of 1.54Å, θ is the Bragg diffraction angle in degrees, k is a fixed number of 0.9 and β is the FWHM of (002) plane. The grain sizes were found to be 14.62, 22.53 and 32.74 nm for the films annealed at 250,350 and 450^{o}C. By increasing the annealing temperature the grain size of the ZnO thin films gets increased and good grain size was obtained at 450^{o}C.

Morphological studies

Figure 2 (a-d) show the SEM images of ZnO thin films annealed at 250, 350, and 450^{o}C. By increasing the annealing temperature, the grains become denser and larger which can be considered as a coalescence process induced by the thermal treatment. For ZnO nanoparticles, there are many Frenkel defects, such as Zn interstitials and oxygen vacancies at grain boundaries[31,32]. As a result, these defects are favorable to coalescence process to make larger grains with an increase in the annealing temperature[32]. These results are in agreement with the XRD analysis. The crystalline size increases with increasing annealing temperature from 250 to 450^{o}C. Film annealed at 450^{o}C shows the structure is consisting of spherical grains of different sizes, uniformly dispersed throughout the film. The particles with a size range of 0.4 to 0.51µm have well defined boundaries. As the annealing temperature increases the porosity of the film get increased and the thin film prepared at 450^{o}C shows a higher porosity.

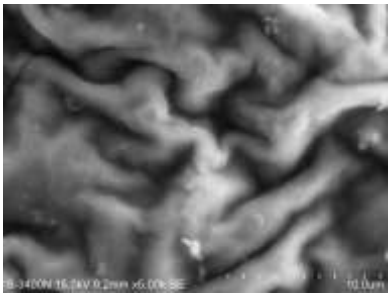

Figure 2 : (a) as prepared ZnO thin film.

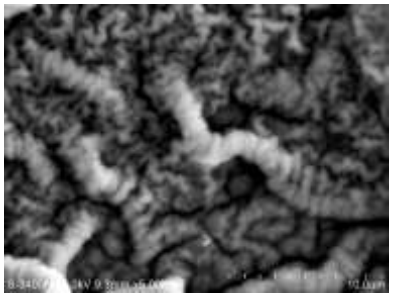

Figure 2 :(b) ZnO thin film annealed at 250^{o}C.

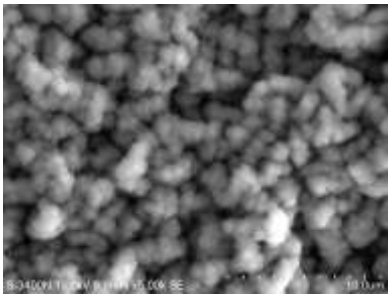

Figure 2 :(c) ZnO thin film annealed at 350^{o}C.

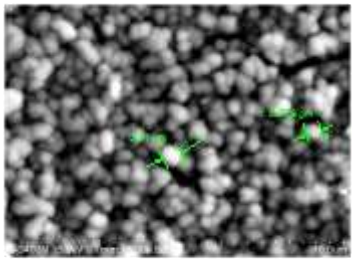

Figure 2 :(d) ZnO thin film annealed at 450°C.

Optical properties

The optical absorption spectra of ZnO thin films annealed at 250, 350, and 450°C is shown in the Figure 3.The absorbance intensity of the UV peaks increases with increase in the annealing temperature from 250 to 450°C and sharp peaks with maximum absorption intensity in UV region were observed for the film annealed at 450°C.

The absorption below 400 nm is assigned to the intrinsic band gap absorption of ZnO, due to electron transition from the valance band to conduction band. The absorption edge shifts to higher wavelength with increase of annealing temperature. The optical band gap of ZnO films was found to decrease with the increase in annealing temperature. The optical band gaps were found to be 3.28, 3.24 and 3.22 eV for the films annealed at 250,350 and 450°C. The decrease in band gap of ZnO films may be attributed to the improvement in the crystalline quality of the films and increase in grain size.

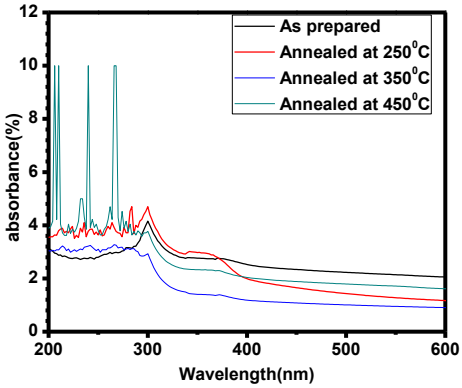

Figure 3. UV-Vis absorption spectra of the ZnO thin films annealed at different temperatures.

Figure 4 shows the PL spectra of ZnO thin films annealed at 250, 350, and 450°C for emission energy ranging from 1.8 to 3.4eV. It may be observed that all the PL spectra are dominated by strong luminescence peak at ~3.22eV followed by peak at ~2.4eV. The UV peak is attributed to the recombination of free excitons through excion - exciton collision process due to the 3.22 eV (382) wide direct band gap transition of ZnO, and therefore indicates good crystallinity of ZnO samples. The sample annealed at 250,350 and 450°C are showing visible emission centered at ~2.4eV. With increase in annealing temperature, the intensity of the visible emission gets increased and shift towards the higher energy side and all the annealed samples show green emission band centered at ~2.4eV. The strong green emission (550 nm) resulted primarily from intrinsic defects. The intrinsic defects are associated with deep level emissions such as oxygen vacancies and interstitials[27,33]. The oxygen vacancies and interstitials were induced by the thermal treatment process and sol-gel process.

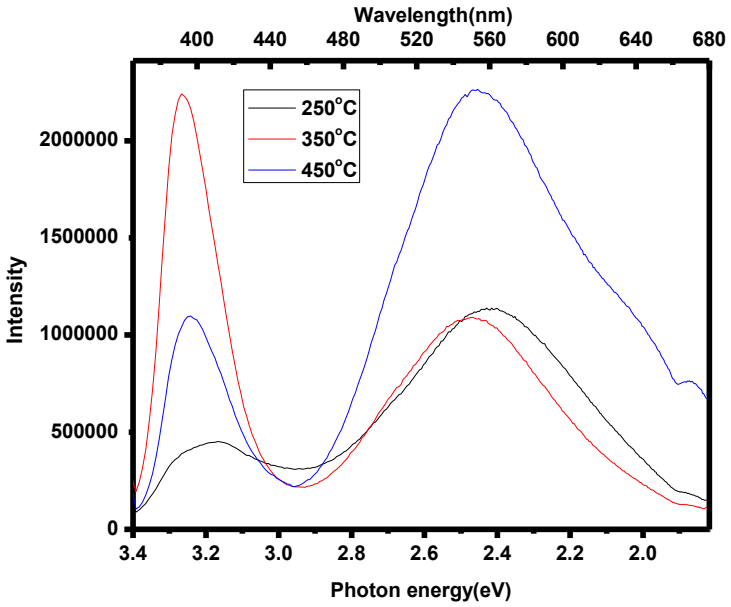

Figure 4. Photoluminescence spectra of ZnO thin films annealed at different temperatures.

The broad emission band revealed in the visible region is due to the superposition of green and yellow emission. The green emission is typically associated with oxygen vacancy and the yellow emission is associated with interstitial oxygen. The two oxygen defects are competing with each other, presenting in the competition of green and yellow bands in PL. These two oxygen defects, can enhance the electron hole pair separation rate in ZnO thin films. As the redox reactions might occur on the surface of oxygen vacancies and interstitial oxygen defects, the oxygen defects can be considered to be the active sites of the ZnO photocatalyst [34]. The obtained PL results reveal that the films annealed at 450°C exhibit broad and strong green and yellow emission and this is due to oxygen vacancies and interstitial oxygen defects.

From the above discussion, it was clearly observed that the ZnO thin films annealed at 450°C result in good crystallinity and grain size, higher porosity, maximum UV absorbance and smaller optical band gap. From the PL, we can conclude that films annealed at 450°C have good number of oxygen vacancies and interstitial defects. From these results it is clear that one can apply these high quality ZnO thin films as photocatalysts in photocatalytic decolorization of organic contaminants.

Photocatalytic activity test

Methyelene blue($C_{16}H_{18}N_3SCI$), a widely used dye, was employed as a representative dye pollutant to evaluate the photocatalytic activity of ZnO thin films. The samples were suspended in 20ml methyelene blue solution (5ppm) and were irradiated with 8W UV lamp placed at a distance of 4.0 cm. The photocatalytic activity was studied by varying the irradiation time and area.

Hence activation of the ZnO surface with UV radiation results in the promotion of the valence band electron to the conduction band, generating electron / hole pairs. The electrons then react with oxygen in the sample to form O_2• and holes react with surface hydroxyl groups to form OH• radicals. The radical species then attack the organic molecule which is eventually oxidized to CO_2 and H_2O. The mechanism of ZnO-photocatalyzed reactions has been a subject of extensive research. Although the detailed mechanism differs from one pollutant to another, it has been widely recognized that hydroxyl radical •OH acts as active reagent for the mineralization of organic compounds.

$ZnO + h\upsilon \rightarrow ZnO^* (e_{CB}^- + h_{VB}^+)$

Formation of electron-hole pair

$hVB^+ + Dye \rightarrow$ direct oxidated dye

$hVB^+ + H_2O \rightarrow H^+ + {}^{\bullet}OH$

formation of hydroxyl radial

$hVB^+ + {}^-OH \rightarrow {}^{\bullet}OH$

formation of hydroxyl radical

Electrons in the conduction band (e_{CB}^-) on the catalyst surface can reduce molecular oxygen to superoxide anion which in turn, can lead to generation of H_2O_2 through a series of redox reactions

$e_{CB}^- + O_2 \rightarrow {}^{\bullet}O_2^-$

$O_2^- + H^+ \rightarrow HO_2^{\bullet}$

$HO_2^{\bullet} + HO_2^{\bullet} \rightarrow H_2O_2 + O_2$

${}^{\bullet}O_2^- + HO_2^{\bullet} \rightarrow HO_2^- + O_2$

$HO_2^- + H^+ \rightarrow H_2O_2$

The photo generated hydrogen peroxide undergoes further decomposition to yield hydroxyl radicals

$H_2O_2 + O_2 \rightarrow OH\bullet + OH\bullet + O_2$

$H_2O_2 + e^- \rightarrow HO\bullet + OH^-$

Direct participation of the holes and electrons in oxidation / reduction reactions

$H_2O_2 + h\nu \rightarrow .OH + .OH$

$.OH$ + dye → dye intermediate

$.OH$ + dye intermediate → $CO_2 + H_2O$ + end products [35, 36].

The absorbance of the methyelene blue solution was measured at intervals of 1 hour and the total irradiation time is 4 hour. The absorbance of the peak at 665nm is used to evaluate the absorbance of methyelene blue solution. The photocatalytic degradation could be evaluated by measuring the absorbance of the solution at 665nm.

Loss of intensity and shift in this peak position was considered as degradation of methylene blue. The percentage degradation (% D) was calculated using formula

Percentage of degradation = $\frac{A_o - A_t}{A_t} X100$

Where A_0 = absorbance at t = 0 minute

A_t = absorbance at t minute.

Figure. 5 shows the time dependent UV–Vis absorbance spectra of methyelene blue dye during photo irradiation with ZnO thin films. The rate of decolorization was recorded with respect to the change in the intensity of absorption peak in visible region. The prominent peak was observed at 665 nm which decreased gradually with increase in irradiation time from 1 hour, 2 hour, 3 hour and 4 hour indicating that the dye had been degraded. The degradation efficiency of ZnO thin films prepared at 450^0C was found to increase from 31.48%, 55.25%, and 70.63% to 84.55% respectively for the irradiation time of 1hour, 2hour, 3 hour and 4hour.

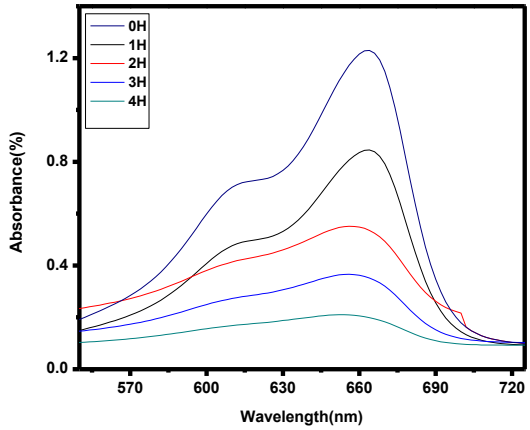

Figure 5. Time-dependent UV–Vis absorption spectra for decolorization of methyelene blue using ZnO thin film.

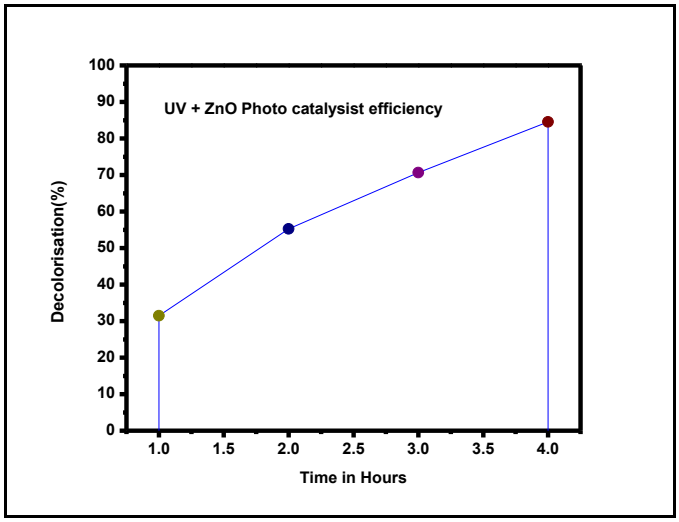

Figure 6. Photo catalytic de-colorization of methelene blue dye with various irradiation time

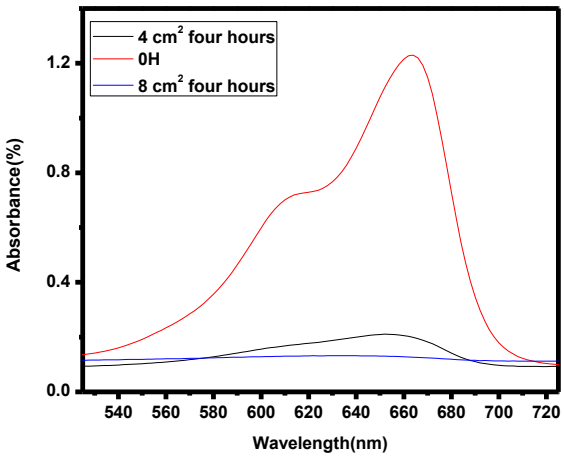

Figure 7. Area-dependent UV–Vis absorption spectra for decolorization of methyelene blue using ZnO thin film.

Figure 6 shows the effect of irradiation time on the de-colorization of methelene blue. It can be seen that the de-colorization of the dye gets gradually increased by increasing the irradiation time from 1hour, 2hour, 3 hour and 4 hour for MB.

Figure. 7 shows the area dependent UV–Vis absorbance spectra of MB dye during photo irradiation with ZnO thin films. The area of the ZnO thin films was varied and dipped in MB and exposed to UV-light. The prominent peak was observed at 665 nm which decreases gradually with increase in irradiation area. The absorbance observed at 665 nm has been decreased gradually with increase in area of the catalyst from 4cm^2 to 8cm^2, indicating the degradation of the dye. When the mixture of ZnO thin films and MB was exposed to UV-light with variation in the area of the catalyst, 90.24% decomposition of MB was recorded for 8cm^2.

The decolorization of dye was achieved as 84.5% and 90.24 % for the variation in area of the catalyst from 4 cm^2 to 8 cm^2. Fig 9 shows the effect of area of catalyst on the decolorization of methelene blue. The results indicate that ZnO exhibits higher photo catalytic activity when irradiation time and area of catalyst is increased for the decolorization of MB.

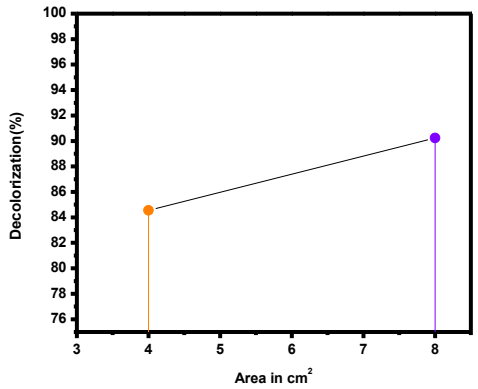

Figure 8. Photo catalytic decolorization of methelene blue dye with varying area of catalyst

Conclusion

In this present work, we have reported a simple spin coating route to synthesize the ZnO thin films. It has been found that annealing temperature significantly influences grain size, crystallinity, morphology and band gap when the annealing temperature was increased from 250 to 450^{0}C. The UV- Vis absorbance spectra indicate that the intensity of the UV peaks increases with increase in the annealing temperatures and sharp peaks with maximum intensity in UV region are observed at 450^{o}C.The PL spectra show that the intensity of the visible emission of the thin films increases with increasing annealing temperature. The maximum intensity is in green and yellow region at 450^{o}C which are typically associated with oxygen vacancies and interstitial oxygen defects. The ZnO thin films annealed at 450^{o}C were used as effective catalysts for photo degradation of methylene blue in water under UV irradiation and it is found that their inherent oxygen defects lead to enhancement in photocatalytic efficiency. A maximum photo degradation efficiency of 90.24% is reported.

References

1. Y. Wang, Y. He, T. Li, J. Cai, M. Luo and L.Zhao, Catal. Commun., 18(2012) 161-64.
2. M.N. Rashed and a.A. El-Amin, Int.J.Phys. Sci., 2(2007) 073-081.
3. W.S. Chiu, P.S. Khiew, M.Cloke, D.Isa, T.K. Tan, S.Radiman, R.Abd-Shukor, M.A. Abd. Hamid, N .M. Huang, H.N. Lim and C.H. Chia, Chem. Eng. J., 158 (2010) 345-352.
4. N.S. Anwar, A. Kassim, H.N. Lim, S.A. Zakarya and N.M. Huang, Sains Malaysiana, 39 (2010) 261-265.
5. S.A. Zakarya, A. Kassim, H.N. Lim, N.S. Anwar and N.H. Huang, Sains Malaysiana, 39 (2010) 975-979.

6. P. Zu, Z.K. Tang, G.K.L. Wong, M. Kawasaki, A. Ohtomo, H. Koinuma, Y. Segawa, (1997) Solid State Commun. 103, 459.
7. E. Ohshima, H. Ogino, I. Niikura, K. Maeda, M. Sato, M. Ito, T. Fukuda, (2004) J. Cryst. Growth 260, 166.
8. T.L. Yang, D.H. Zhang, J. Ma, H.L. Ma, Y. Chen, (1998) Thin Solid Films 326, 60.
9. B. Sang, A. Yamada, M. Konagai, (1998) Jpn. J. Appl. Phys. 37, L 206.
10. J.F. Cordaro, Y. Shim, J.E. May, (1986) J. Appl. Phys. 60, 4186.
11. P.Verardi, N.Nastase, C. Gherasim, C.Ghica, M. Dinescu, R. Dinu,C. Flueraru, (1999) J. Cryst. Growth 197, 523.
12. K Byrappa, A K Subramani, S Ananda, K M Lokanatha Rai, R Dinesh , M Yoshimura

a. (2006) Bull. Mater. Sci., Vol. 29, No. 5, pp. 433–438.

13. Y.X.Wang, X.Y.Li, G.Lu, X. Quan, G.H.Chen, J. Phys. Chem. C 112 (2008) 7332.
14. Q. Wan, T.H. Wang, J.C. Zhao appl. Phys. Lett. 87 (2005) 083105.
15. Y.H. Tong, J. Cheng, Y.L. Liu, G.G. Siu, Scripta Mater. 60 (2009) 1093.
16. M. Dutta, D. Basak, Nanotechnology 20 (2009) 1147.
17. F.Quaranta, A. Valentini, f.R. Rizzi, Dual-ion-beam sputter deposition of ZnO films, *J. Appl. Phys*. 74 (1993) 247-248.
18. V. Cracium, J. Elderss, J.G.E. Gardeniers, Characterisitics of highe quality ZnO thin films deposited by pulsed laser deposition, *Appl. Phys. Lett.* 65 (1994) 2963-2965.
19. C.K. Ong, S.J. Wang, In situ RHEED monitor of the growth of epitaxial anatase TiO_2 thin films, *Appl. Surf. Sci*. 185 (2001) 47-51.
20. A. Kuroyanagi, Properties of aluminum-doped ZnO thin films grown by electron beam evaporation, *Jpn. J. Appl. Phys*. 28 (1989) 219-222.
21. A.J.C. Fiddes, K. Durose, A.W. Brinkman, Preparation of ZnO films by spray pyrolysis, *J. Cryst. Growth* 159 (1996) 210-213.
22. M. Ohyama, H. Kozuka, T. Yoko, Sol-gel preparation of ZnO films with extremely preferred orientation along (0 0 2) plane from zinc acetate solution, *Thin Solid Films* 306 (1997) 78-85.
23. D. Bao, H.Gu, A. Kuang, Sol-gel derived c-axis oriented ZnO thin films, *Thin Solid Films* 312 (1998) 37-39.
24. H.C. Han, I.-J. Kim, W.-P. Tai, J,-K. Kim, M.S. Shim, S.-J. Suh, Y.-S. Kim, Structural, optical, electrical properties of ZnO thin films with zn concentration, J. *Korean Ceram. Soc*. 40 (2003) 1113-1119.
25. I.-J. Kim, H.-C. Han, C.-S. Lee, Y.-J Song, W.-P. Tai, S.-J. Suh, Y.-S. Kim, Physical properties of ZnO thin films grown by sol- gel process with different preheating temperatures, *J. Korean Ceram. Soc.* 41 (2004) 136-142.
26. S.Muthukrishnan, T.A.Venkatsubramaniam, Thin Film Solar Cells Novel Approaches by Different Method of Techniques, International Journal of Chemical Concepts, 2015, 1 (3), 149-153.
27. R.H. Bari, Selectivity of organic vapour for nanostructured CdO thin films prepared by sol-gel dip coating technique, International Journal of Chemical Concepts, 2015, 1 (3), 136-148.
28. R. H. Bari, S. B. Patil Improved NO_2 sensing performance of nanostructured Zn doped SnO_2 thin films, International Journal of Chemical Concepts, 2015, 1 (2), 86-96.
29. R. H. Bari S. B. Patil Ethanol sensing performance of nanostructured Zn doped $CdSnO_3$ thin films International Journal of Chemical Concepts, 2016, 2 (1), 01-11.
30. C.J .Brinker, G.W. Scherer, Sol-Gel Science: The physics and Chemistry of Sol-Gel Processing, *Academic Press, New York*, 1990.
31. Biju, K.P. and Jain, M.K. , Thin Solid Films, Vol.516, pp. 2175-2180, (2008).
32. Zhi Z.Z., Liu Y.c., Li B.S., Zhang X.T., Lu Y.M., Shen D.Z., Fan X.W. J. Phys. D : Appl. Phys, 36, 719-722,(2003).
33. Pearton. SJ., Norton D P., Ip K, Heo YW., Steiner.T. Superlattices and Microstructures , 34 (1), 3-32 (2003).
34. Vanheusden K., Warren W. L., Seager C. H., Tallant D. R., Voigt J. A., Gnade B. E. Journal of Applied Physics, 79, 7983-79(1996.).
35. Wang J., Liu P., Fu X., li Z., Han W., Wang X., Langmuir , 25 ,1218-1223(2009).
36. So-Jung Kim and Dong-Wha Park,Applied Surface Science., 225:5363(2009)

*****